Thermal, Non-thermal dark matter and their detection

Sarif Khan

Harish-Chandra Research Institute, Allahabad, India

Talk at: MPIK, Heidelberg

November 5, 2018

Talk Plan

- Motivation

Talk Plan

- Motivation
- DM Evidences

Talk Plan

- Motivation
- DM Evidences
- Thermal DM

Talk Plan

- Motivation
- DM Evidences
- Thermal DM
- Non-thermal DM

Motivation

- Discovery of neutrino oscillation implies the existence of neutrino mass.

Motivation

- Discovery of neutrino oscillation implies the existence of neutrino mass.

✓ Almost 80% matter contents of the universe is unknown to us, namely Dark Matter (DM) [Many evidences which support the presence of DM].

Motivation

- Discovery of neutrino oscillation implies the existence of neutrino mass.

✓ Almost 80% matter contents of the universe is unknown to us, namely Dark Matter (DM) [Many evidences which support the presence of DM].

- Why there exist excess matter over antimatter in the universe.

Motivation

- Discovery of neutrino oscillation implies the existence of neutrino mass.
- ✓ Almost 80% matter contents of the universe is unknown to us, namely Dark Matter (DM) [Many evidences which support the presence of DM].
- Why there exist excess matter over antimatter in the universe.
- Disagreement between the theoretical and experimental value of muon $(g-2)$.

Evidences

1. Galaxy Clusters:

Figure: Coma Cluster

- In 1933, Fritz Zwicky was studying the nearest Coma Cluster.

Evidences

1. Galaxy Clusters:

Figure: Coma Cluster

- In 1933, Fritz Zwicky was studying the nearest Coma Cluster.
- Using Virial theorem (which relates the KE and PE), he determined the Gravitational mass (GM).

Evidences

1. Galaxy Clusters:

Figure: Coma Cluster

- In 1933, Fritz Zwicky was studying the nearest Coma Cluster.
- Using Virial theorem (which relates the KE and PE), he determined the Gravitational mass (GM).
- Compared GM with the bright, luminous mass, got discrepancy.

Evidences

1. Galaxy Clusters:

Figure: Coma Cluster

- In 1933, Fritz Zwicky was studying the nearest Coma Cluster.
- Using Virial theorem (which relates the KE and PE), he determined the Gravitational mass (GM).
- Compared GM with the bright, luminous mass, got discrepancy.
- Concluded that, extra matter is there and called it “Dark Matter”.

Evidences

2. Galactic Rotation Curve:

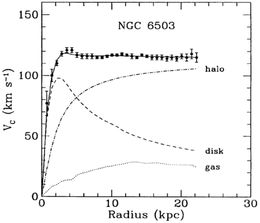

Figure: GC rotation curve

- Vera Rubin and Kent Ford were studying Andromeda galaxy in 1960, got similar things.

Evidences

2. Galactic Rotation Curve:

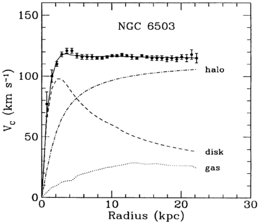

Figure: GC rotation curve

- Vera Rubin and Kent Ford were studying Andromeda galaxy in 1960, got similar things.
- Velocity of the stars remained almost constant regardless of how far they are from GC. [Small: $v(r) \propto r$, Large: $v(r) \propto \frac{1}{\sqrt{r}}$]

Evidences

2. Galactic Rotation Curve:

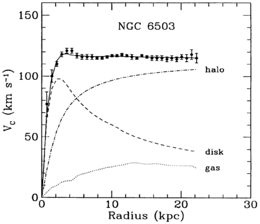

Figure: GC rotation curve

- Vera Rubin and Kent Ford were studying Andromeda galaxy in 1960, got similar things.
- Velocity of the stars remained almost constant regardless of how far they are from GC. [Small: $v(r) \propto r$, Large: $v(r) \propto \frac{1}{\sqrt{r}}$]
- Excess matter is present, namely DM. (Another way: MOND theory!)

3. CMB Spectrum:

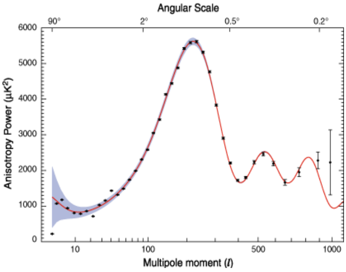

Figure: CMB Spectrum

- CMB Power Spectrum has been measured by the WMAP and Planck.

3. CMB Spectrum:

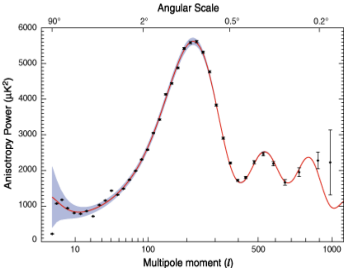

Figure: CMB Spectrum

- CMB Power Spectrum has been measured by the WMAP and Planck.
- From spectrum we come to know:
  Baryon density: $\Omega_b h^2 \simeq 0.02$
  DM density: $\Omega_{DM} h^2 \simeq 0.1203$
  Hubble Parameter: $H_0 \simeq 67.11$ MPc^{-1} s^{-1} ($\tau_U \sim 13.819$ Gy).

Evidences

4. Bullet Cluster:

Figure: Bullet Cluster

- In Bullet-Cluster, X-ray emission and gravitational lensing are used.

Evidences

4. Bullet Cluster:

Figure: Bullet Cluster

- In Bullet-Cluster, X-ray emission and gravitational lensing are used.
- Red regions are obtained by the X-ray emission and the blue regions by the gravitational lensing.

Evidences

4. Bullet Cluster:

Figure: Bullet Cluster

- In Bullet-Cluster, X-ray emission and gravitational lensing are used.
- Red regions are obtained by the X-ray emission and the blue regions by the gravitational lensing.
- center of the total matter and the visible matter does not coincide, hence DM is present.

Evidences and Attempts

- Large-Scale Structure Formation: SDSS telescope when maps to large scale, it sees some patterns which can not be explained just by the ordinary matter.

Evidences and Attempts

- Large-Scale Structure Formation: SDSS telescope when maps to large scale, it sees some patterns which can not be explained just by the ordinary matter.
- Since, DM only interacts via gravity, hence we can tackle this by modifying gravity like MOND theory, but it can not explain all except flatness of rotation curve (Although gravity is well known to us by GR, e.g. GPS system).

Evidences and Attempts

- Large-Scale Structure Formation: SDSS telescope when maps to large scale, it sees some patterns which can not be explained just by the ordinary matter.
- Since, DM only interacts via gravity, hence we can tackle this by modifying gravity like MOND theory, but it can not explain all except flatness of rotation curve (Although gravity is well known to us by GR, e.g. GPS system).
- Another possibility was MACHO type objects (e.g. neutron stars, and brown and white dwarfs), possible to detect by the Gravitational lensing. But failed to explain the entire amount of DM.

Evidences and Attempts

- Large-Scale Structure Formation: SDSS telescope when maps to large scale, it sees some patterns which can not be explained just by the ordinary matter.
- Since, DM only interacts via gravity, hence we can tackle this by modifying gravity like MOND theory, but it can not explain all except flatness of rotation curve (Although gravity is well known to us by GR, e.g. GPS system).
- Another possibility was MACHO type objects (e.g. neutron stars, and brown and white dwarfs), possible to detect by the Gravitational lensing. But failed to explain the entire amount of DM.
- From BBN and CMB, we know the amount of baryonic matter present in the universe, hence DM will be non baryonic.

Particle Dark Matter

I will discuss DM from particle physics point of view,

- Easy to explain everything with the particle DM.

Particle Dark Matter

I will discuss DM from particle physics point of view,

- Easy to explain everything with the particle DM.
- Theoretically well motivated and also testable at the satelite and earth based experiments.

Particle Dark Matter

I will discuss DM from particle physics point of view,

- Easy to explain everything with the particle DM.
- Theoretically well motivated and also testable at the satelite and earth based experiments.
- Many theories are there: SUSY, Extra dimensions, heavy neutrinos, MeV DM, Axion, Fermionic and Scalar DM...

I will discuss DM from particle physics point of view,

- Easy to explain everything with the particle DM.
- Theoretically well motivated and also testable at the satelite and earth based experiments.
- Many theories are there: SUSY, Extra dimensions, heavy neutrinos, MeV DM, Axion, Fermionic and Scalar DM...
- I will focus on the **Fermionic DM**, by conidering its **thermal and non-thermal** ways of production.

Thermal Dark Matter

- "Singlet-Triplet Fermionic Dark Matter and LHC Phenomenology", S. Choubey, **S.K.**, M. Mitra and S. Mondal, Eur. Phys. J. C **78**, no. 4, 302 (2018) [arXiv:1711.08888 [hep-ph]].

Strategy in thermal DM Study

In discussing DM, I will be focusing on the following points

- Satisfying Relic Density bound.

Strategy in thermal DM Study

In discussing DM, I will be focusing on the following points

- Satisfying Relic Density bound.
- DM direct detection.

Strategy in thermal DM Study

In discussing DM, I will be focusing on the following points

- Satisfying Relic Density bound.
- DM direct detection.
- DM indirect detection.

Strategy in thermal DM Study

In discussing DM, I will be focusing on the following points

- Satisfying Relic Density bound.
- DM direct detection.
- DM indirect detection.
- DM collider signature.

Standard Model Particles

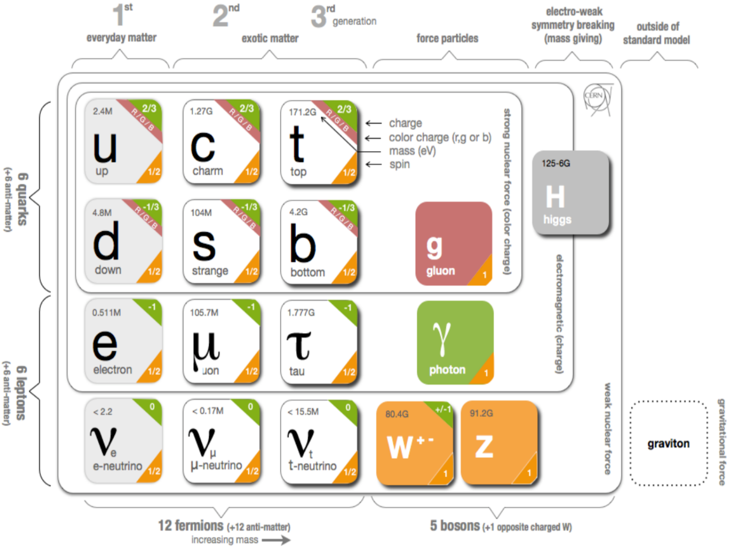

♣ Need to extend the SM.

♣ Need to extend the SM.

♣ One of the Simplest extension is to introduce a triplet fermion,

Gauge Group	Baryon Fields			Lepton Fields			Scalar Fields
	$Q_L^i = (u_L^i, d_L^i)^T$	u_R^i	d_R^i	$L_L^i = (\nu_L^i, e_L^i)^T$	e_R^i	ρ	ϕ_h
$SU(3)_c$	3	3	3	1	1	1	1
$SU(2)_L$	2	1	1	2	1	3	2
$U(1)_Y$	1/6	2/3	−1/3	−1/2	−1	0	1/2
$\mathbb{Z}_2$	+	+	+	+	+	−	+

where

$$\rho = \begin{pmatrix} \frac{\rho_0}{2} & \frac{\rho^+}{\sqrt{2}} \\ \frac{\rho^-}{\sqrt{2}} & -\frac{\rho_0}{2} \end{pmatrix} .$$

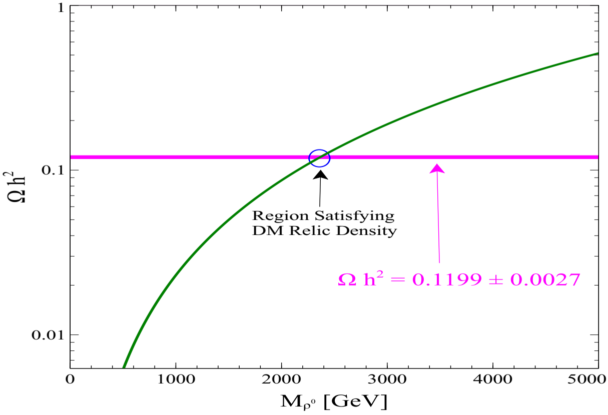

♠ Relic density satisfies around 2.3 TeV.

Relic Density

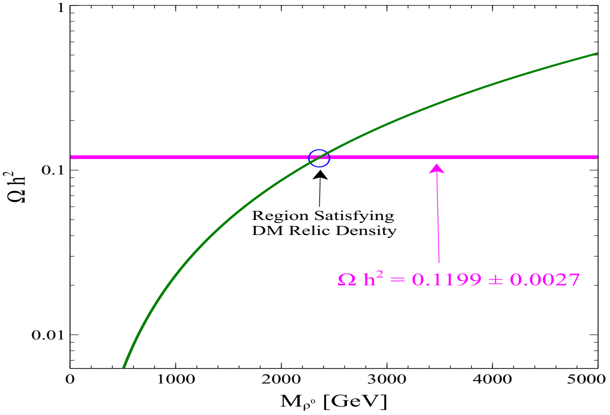

- ♠ Relic density satisfies around 2.3 TeV.
- ♠ This simplest model has few drawbacks which are as follows.

Drawbacks

- Relic density satisfies around 2.3 TeV. Difficult to produce and detect such High mass DM at the current energy range of LHC.

Drawbacks

- Relic density satisfies around 2.3 TeV. Difficult to produce and detect such High mass DM at the current energy range of LHC.
- No tree level DD processes exist and only possible via one loop, hence SIDD is suppressed.

Cont...

J. Hisano et. al. [PRD 05]

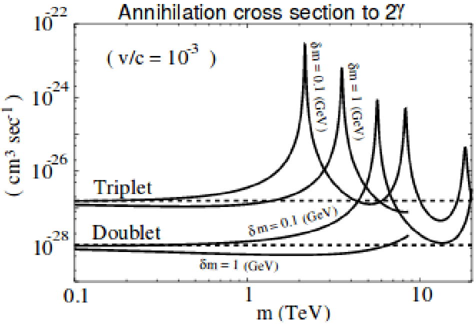

- Annihilation gets Sommerfeld enhancement after mass greater than 1 TeV.

Cont...

J. Hisano et. al. [PRD 05]

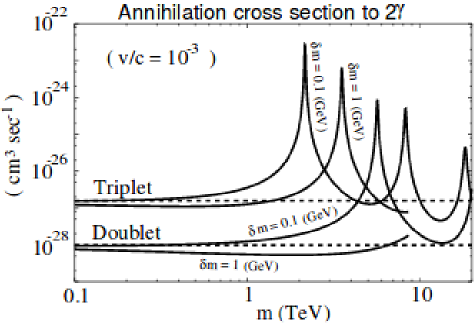

- Annihilation gets Sommerfeld enhancement after mass greater than 1 TeV.
- Pure triplet DM is ruled out by the HESE and Fermi-LAT data which give bound on the $\gamma\gamma$ channel.

Way Out

- One way out is to introduce a Singlet fermion and triplet scalar.

Way Out

- One way out is to introduce a Singlet fermion and triplet scalar.
- Complete particles list are as follows,

Gauge	Baryon Fields			Lepton Fields				Scalar Fields	
Group	$Q_L^i = (u_L^i, d_L^i)^T$	u_R^i	d_R^i	$L_L^i = (\nu_L^i, e_L^i)^T$	e_R^i	N'	ρ	ϕ_h	Δ
$SU(3)_c$	3	3	3	1	1	1	1	1	1
$SU(2)_L$	2	1	1	2	1	1	3	2	3
$U(1)_Y$	1/6	2/3	−1/3	−1/2	−1	0	0	1/2	0
$\mathbb{Z}_2$	+	+	+	+	+	−	−	+	+

Way Out

- One way out is to introduce a Singlet fermion and triplet scalar.
- Complete particles list are as follows,

Gauge Group	Baryon Fields			Lepton Fields				Scalar Fields	
	$Q_L^i = (u_L^i, d_L^i)^T$	u_R^i	d_R^i	$L_L^i = (\nu_L^i, e_L^i)^T$	e_R^i	N'	ρ	ϕ_h	Δ
$SU(3)_c$	3	3	3	1	1	1	1	1	1
$SU(2)_L$	2	1	1	2	1	1	3	2	3
$U(1)_Y$	1/6	2/3	−1/3	−1/2	−1	0	0	1/2	0
$\mathbb{Z}_2$	+	+	+	+	+	−	−	+	+

- Will see, after adding two particles all the above drawbacks are solved.

Lagrangian

- Lagrangian for the present model is given by,

$$\begin{aligned}\mathcal{L} &= \mathcal{L}_{SM} + Tr\left[\bar{\rho}\, i\,\gamma^{\mu} D_{\mu}\,\rho\right] + \bar{N'}\, i\,\gamma^{\mu} D_{\mu} N' + Tr[(D_{\mu}\Delta)^{\dagger}(D^{\mu}\Delta)] - V(\phi_h, \Delta) \\ & -Y_{\rho\Delta}\,(Tr[\bar{\rho}\,\Delta]\,N' + h.c.) - M_{\rho}\; Tr[\bar{\rho^c}\,\rho] - M_{N'}\;\bar{N'^c}N'\end{aligned}$$

where the triplet fermion takes the following form,

$$\rho = \begin{pmatrix} \frac{\rho_0}{2} & \frac{\rho^+}{\sqrt{2}} \\ \frac{\rho^-}{\sqrt{2}} & -\frac{\rho_0}{2} \end{pmatrix} .$$

Lagrangian

- Lagrangian for the present model is given by,

$$\begin{aligned}\mathcal{L} &= \mathcal{L}_{SM} + Tr\left[\bar{\rho}\, i\,\gamma^{\mu} D_{\mu}\rho\right] + \bar{N'}\, i\,\gamma^{\mu} D_{\mu} N' + Tr[(D_{\mu}\Delta)^{\dagger}(D^{\mu}\Delta)] - V(\phi_h, \Delta) \\ &\quad - Y_{\rho\Delta}\,(Tr[\bar{\rho}\,\Delta]\, N' + h.c.) - M_{\rho}\; Tr[\bar{\rho^{c}}\,\rho] - M_{N'}\; \bar{N'^{c}} N'\end{aligned}$$

where the triplet fermion takes the following form,

$$\rho = \begin{pmatrix} \frac{\rho_0}{2} & \frac{\rho^{+}}{\sqrt{2}} \\ \frac{\rho^{-}}{\sqrt{2}} & -\frac{\rho_0}{2} \end{pmatrix} .$$

- The complete form of the potential $V(\phi_h, \Omega)$ takes the following form,

$$\begin{aligned}V(\phi_h, \Delta) &= -\mu_h^2 \phi_h^{\dagger}\phi_h + \frac{\lambda_h}{4}(\phi_h^{\dagger}\phi_h)^2 + \mu_{\Delta}^2\, Tr[\Delta^{\dagger}\Delta] + \lambda_{\Delta}(\Delta^{\dagger}\Delta)^2 + \lambda_1\,(\phi_h^{\dagger}\phi_h)\,\mathrm{Tr}\,[\Delta^{\dagger}\Delta] \\ &\quad + \lambda_2\, \left(Tr[\Delta^{\dagger}\Delta]\right)^2 + \lambda_3\; Tr[(\Delta^{\dagger}\Delta)^2] + \lambda_4\; \phi_h^{\dagger}\Delta\Delta^{\dagger}\phi_h + (\mu\phi_h^{\dagger}\Delta\phi_h + h.c.)\,.\end{aligned}$$

Mass Eigenstates

☞ ϕ_h will take vev spontaneously, and simultaneously the triplet scalar Δ will get **induced** *vev*,

$$\mu_h^2 > 0, \quad \mu_\Delta^2 > 0, \quad \lambda_h > 0 \;\; \text{and} \;\; \lambda_\Delta > 0 \,.$$

Mass Eigenstates

- ϕ_h will take vev spontaneously, and simultaneously the triplet scalar Δ will get **induced** *vev*,

$$\mu_h^2 > 0, \quad \mu_\Delta^2 > 0, \quad \lambda_h > 0 \text{ and } \lambda_\Delta > 0\,.$$

- After symmetry breaking, there will be mixing between the **two neutral scalars**, **two charged scalars**, and **two neutral fermions**.

Mass Eigenstates

- ϕ_h will take vev spontaneously, and simultaneously the triplet scalar Δ will get **induced** *vev*,

$$\mu_h^2 > 0, \quad \mu_\Delta^2 > 0, \quad \lambda_h > 0 \;\; \text{and} \;\; \lambda_\Delta > 0\,.$$

- After symmetry breaking, there will be mixing between the **two neutral scalars**, **two charged scalars**, and **two neutral fermions**.
- Therefore, we need to introduce mass basis in the following way,

Neutral Higgs:

$$\begin{aligned} h_1 &= \cos\alpha\, H + \sin\alpha\, \Delta_0 \\ h_2 &= -\sin\alpha\, H + \cos\alpha\, \Delta_0 \end{aligned}$$

Charged Higgs:

$$\begin{aligned} G^\pm &= \cos\delta\, \phi^\pm + \sin\delta\, \Delta^\pm \\ H^\pm &= -\sin\delta\, \phi^\pm + \cos\delta\, \Delta^\pm \end{aligned}$$

Fermions:

$$\begin{aligned} \rho_2^0 &= \cos\beta\, \rho_0 + \sin\beta\, N'^c \\ \rho_1^0 &= -\sin\beta\, \rho_0 + \cos\beta\, N'^c \end{aligned}$$

Constraints Used in DM Study

- **SI direct detection cross section**

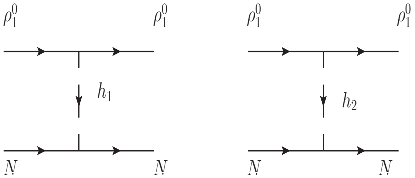

- Direct detection cross section for the Higgses mediated diagrams is,

$$\sigma_{SI} \quad = \quad \frac{\mu_{red}^2}{\pi}\left[\frac{M_N f_N}{v}\frac{\Delta M_{21}\ \sin^2 2\beta\ \sin 2\alpha}{4 v_\Delta}\left(\frac{1}{M_{h_2}^2}-\frac{1}{M_{h_1}^2}\right)\right]^2$$

Contd...

- **Invisible decay width of Higgs [ATLAS + CMS: JHEP 16]** :
  Higgs can decay to DM, if $M_{h_1} > 2M_{\rho_1^0}$ and the constraint is,

$$\frac{\Gamma_{h_1 \to \rho_1^0 \rho_1^0}}{\Gamma_{h_1}^{Total}} \leq 34\% \text{ at } 95\% \text{ C.L.}$$

- **Planck Limit [Planck 15]** :
  Relic density bound on the DM is,

$$0.1172 \leq \Omega h^2 \leq 0.1226 \text{ at } 68\% \text{ C.L.},$$

- We consider the bounds on the masses of $\rho^{\pm}$, ρ_2^0 which can come from the search of Wino like neutralinos and Chargino in the context of SUSY.

Feynman diagrams which take part in DM phenomenology

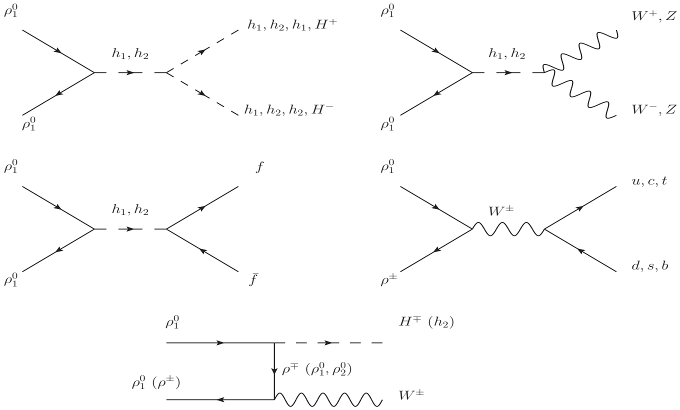

Useful Vertices

- $\rho_1^0 \rho_1^0 h_{1,2}$ vertices look like as follows,

$$\begin{aligned} g_{\rho_1^0 \rho_1^0 h_1} &= \frac{\Delta M_{21} \sin^2 2\beta}{2v} \frac{\sin\alpha}{\tan\delta}, \\ g_{\rho_1^0 \rho_1^0 h_2} &= \frac{\Delta M_{21} \sin^2 2\beta}{2v} \frac{\cos\alpha}{\tan\delta} \end{aligned}$$

  where $\Delta M_{21} = M_{\rho_2^0} - M_{\rho_1^0}$.
- Two important observations:
  - Vertices are proportional to square of the fermionic mixing angle:

$$\begin{aligned} g_{\rho_1^0 \rho_1^0 h_1} &\propto \sin^2\beta \\ g_{\rho_1^0 \rho_1^0 h_2} &\propto \sin^2\beta \end{aligned}$$

  - when $\sin\alpha = \sin\delta$, then

$$\begin{aligned} g_{\rho_1^0 \rho_1^0 h_1} &\propto \cos\alpha \\ g_{\rho_1^0 \rho_1^0 h_2} &\propto 1/\sin\alpha \end{aligned}$$

DM Results

Line Plots :

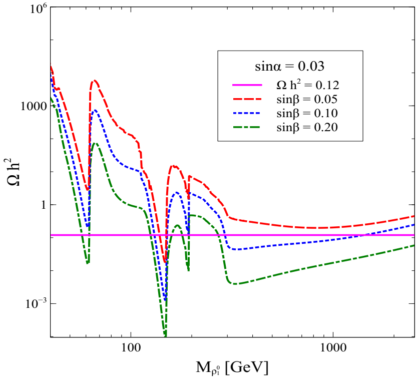

Figure: BSM Higgs mass, $M_{h_2} = 300$ GeV, $\sin\delta = \sin\alpha$ and $\Delta M_{12} = 50$ GeV.

Line Plots :

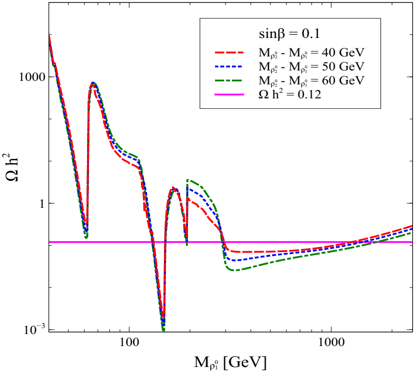

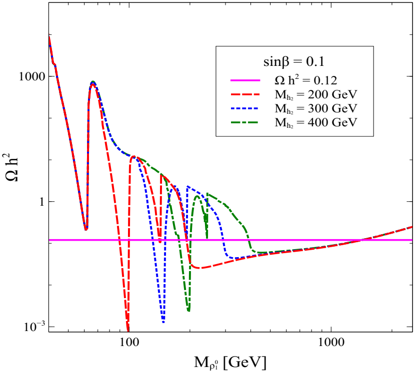

Figure: $\sin\delta = \sin\alpha = 0.03$ and $\Delta M_{12} = 50$ GeV.

Scatter Plots :

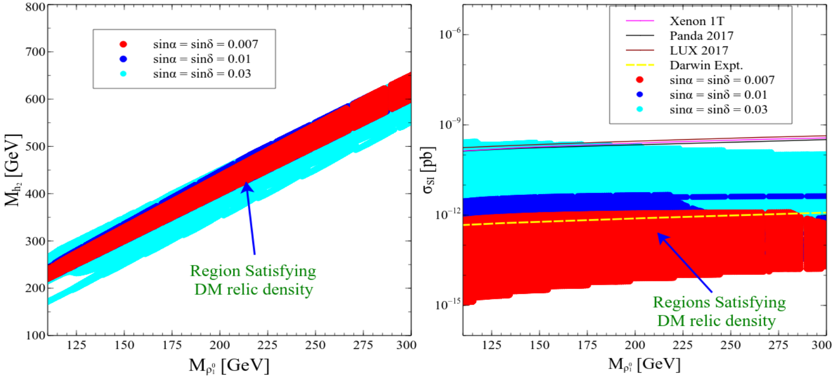

Figure: $M_{\rho_1^0}$, M_{h_2} and $\sin\beta$ three parameters have been varied for scatter plots.

Feynman diagrams contributing in $\gamma\gamma$ final state

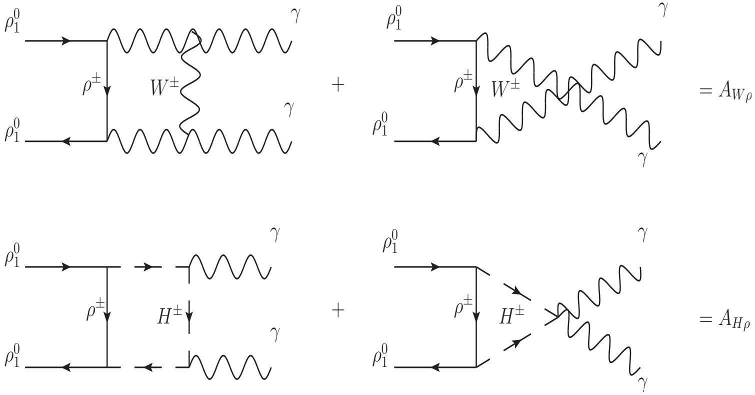

Indirect Detection

- Previous diagrams expression for the CS times velocity is, [L. Bergstrom et. al., NPB 97; Z. Bern et. al, PLB 97]

$$\langle \sigma v \rangle_{\gamma\gamma} = \frac{\alpha_{EM}^2 M_{\rho_1^0}^2}{16\pi^3} |A_{W\rho} + A_{H\rho}|^2 \,.$$

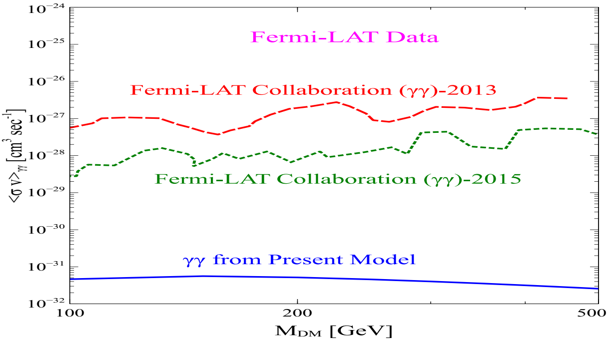

Figure: Fermi-LAT bounds and the prediction from the present model

- **Signal Production** :

$$\begin{aligned} p\,p &\rightarrow X\,Y \\ p\,p &\rightarrow X\,Y\,j \\ p\,p &\rightarrow X\,Y\,j\,j \end{aligned}$$

- **Signal-I**:

$$\{\mathrm{X\ Y}\} = \{\rho_2^0\ \rho^+\},\ \{\rho_2^0\ \rho^-\}$$

- **Signal-II**:

$$\{\mathrm{X\ Y}\} = \{\rho^+\ \rho^-\}$$

- After showering the event by Pythia, we have looked for the following signal,

$$\not{E}_T + n\,j, \textbf{ where n} \geq \mathbf{2}$$

Production cross section at 13 TeV LHC :

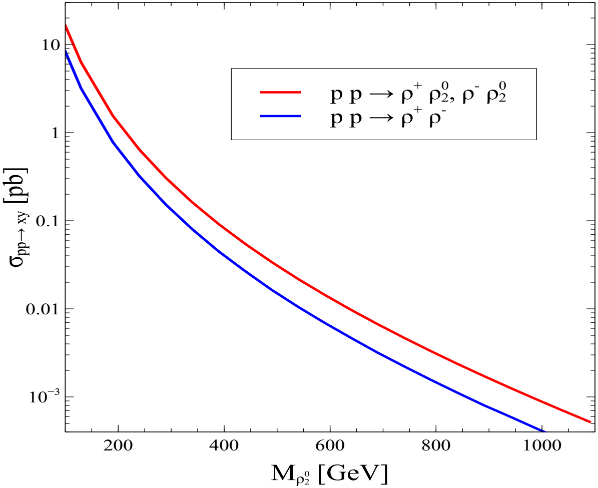

- **Benchmark points**:

Parameters	$M_{\rho_1^0}$ [GeV]	$M_{\rho_2^0}$ [GeV]	M_{ρ^+} [GeV]	M_{h_2} [GeV]	$M_{H^\pm}$ [GeV]	σ_{SI} [pb]	Ωh^2
BP1	87.6	128.0	128.2	195.5	195.5	2.1×10^{-12}	0.1207
BP2	132.0	172.0	172.2	300.0	300.0	4.1×10^{-12}	0.1208
BP3	171.1	211.0	211.2	400.0	400.0	4.8×10^{-12}	0.1197
BP4	86.7	200.0	200.2	194.1	194.1	1.8×10^{-11}	0.1186
BP5	119.0	230.0	230.2	280.0	280.0	2.9×10^{-11}	0.1195

- All the points satisfy relic density, direct and indirect detection bounds.

Histograms for Signal and BKG :

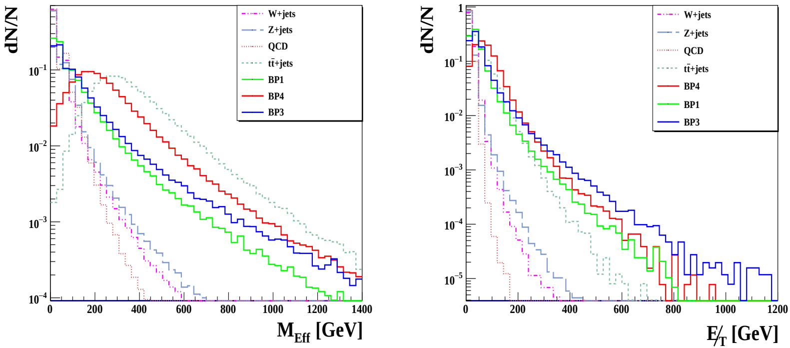

where $\not{E}_T$ is the missing energy and M_{Eff} is defined as,

$$M_{Eff} = \sum_i |\vec{p}^{\,j}_{T_i}| + \sum_i |\vec{p}^{\,\ell}_{T_i}| + \not{E}_T$$

Selection Cuts

Basic Cuts (A0) :

- Leptons are selected with $p_T^l > 10$ GeV and the pseudo rapidity $|\eta^\ell| < 2.5$, where $\ell = e, \mu$.
- We used $p_T^\gamma > 10$ GeV and rapidity $|\eta^\gamma| < 2.5$ as the basic cuts for photon.
- We have chosen the jets which satisfy $p_T^j > 40$ GeV and $|\eta^j| < 2.5$.
- We have considered the azimuthal separation between all reconstructed jets and missing energy must be greater than 0.2 i.e. $\Delta\phi(jet, \vec{\not{E}}_T) > 0.2$.

Selection Cuts

A1: We have imposed a lepton and photon veto in the final state.

Selection Cuts

A1: We have imposed a lepton and photon veto in the final state.

A2: p_T requirements on the hardest and second hardest jets: $p_T^{j_1} > 130$ GeV and $p_T^{j_2} > 80$ GeV.

Selection Cuts

A1: We have imposed a lepton and photon veto in the final state.

A2: p_T requirements on the hardest and second hardest jets: $p_T^{j_1} > 130$ GeV and $p_T^{j_2} > 80$ GeV.

A3: In order to minimize *QCD* multi-jet, we have ensured that the $\vec{\not{E}}_T$ and the jets are well separated, i.e., $\Delta\phi(j_i, \vec{\not{E}}_T) > 0.4$ where i = 1, 2. For all the other jets, $\Delta\phi(j, \vec{\not{E}}_T) > 0.2$.

Selection Cuts

A1: We have imposed a lepton and photon veto in the final state.

A2: p_T requirements on the hardest and second hardest jets: $p_T^{j_1} > 130$ GeV and $p_T^{j_2} > 80$ GeV.

A3: In order to minimize *QCD* multi-jet, we have ensured that the $\vec{\not{E}}_T$ and the jets are well separated, i.e., $\Delta\phi(j_i, \vec{\not{E}}_T) > 0.4$ where i = 1, 2. For all the other jets, $\Delta\phi(j, \vec{\not{E}}_T) > 0.2$.

A4: We demand a hard cut on the effective mass variable, $M_{Eff} > 800$ GeV.

Selection Cuts

A1: We have imposed a lepton and photon veto in the final state.

A2: p_T requirements on the hardest and second hardest jets: $p_T^{j_1} > 130$ GeV and $p_T^{j_2} > 80$ GeV.

A3: In order to minimize *QCD* multi-jet, we have ensured that the $\vec{\not{E}}_T$ and the jets are well separated, i.e., $\Delta\phi(j_i, \vec{\not{E}}_T) > 0.4$ where i = 1, 2. For all the other jets, $\Delta\phi(j, \vec{\not{E}}_T) > 0.2$.

A4: We demand a hard cut on the effective mass variable, $M_{Eff} > 800$ GeV.

A5: We put the bound on the missing energy $\not{E}_T > 160$ GeV.

Cut-flow table for BKG

- **BKG Contribution after applying cuts** :

SM Backgrounds at 13 TeV		Effective Cross section after applying cuts (pb)				
Channels	Cross-section (pb)	$\mathrm{A0+A1}$	A2	A3	A4	A5
$\mathrm{Z} + \leq 4$ jets	5.7×10^{4}	5.5×10^{3}	361.90	241.60	11.40	2.20
$\mathrm{W}^{\pm} + \leq 4$ jets	1.9×10^{5}	9.1×10^{3}	783.20	504.00	18.90	1.50
QCD (≤ 4 jets)	2.0×10^{8}	1.5×10^{7}	3.5×10^{5}	2.4×10^{5}	2.5×10^{3}	-
$t\bar{t} + \leq 2$ jets	722.94	493.73	171.46	120.63	13.89	1.94
$\mathrm{W}^{\pm}\mathrm{Z} + \leq 2$ jets	51.10	19.66	5.37	3.59	0.50	0.12
$\mathrm{ZZ} + \leq 2$ jets	13.71	4.99	0.80	0.53	0.06	0.02
Total Backgrounds						5.78

- QCD BKG is huge, but after M_{Eff} cut it goes to zero.

Cut-flow table for Signal-I

- **Signal-I Contribution after applying cuts** :

Signal at 13 TeV		Effective Cross section after applying cuts (fb)				
BP	Cross-section (pb)	A0 + A1	A2	A3	A4	A5
BP1	6.757	1005.05	175.08	138.45	22.02	19.15
BP2	2.279	385.22	69.16	56.51	11.87	10.85
BP3	1.052	189.71	34.63	29.19	7.36	6.82
BP4	1.296	1047.86	145.67	116.94	14.19	9.82
BP5	0.760	616.00	89.60	72.63	9.80	7.40

Cut-flow table for Signal-II

- **Signal-II Contribution after applying cuts** :

Signal at 13 TeV		Effective Cross section after applying cuts (fb)				
BP	Cross-section (pb)	$A0 + A1$	A2	A3	A4	A5
BP1	3.419	2639.30	74.36	59.18	8.54	7.31
BP2	1.156	880.60	28.77	23.87	4.95	4.43
BP3	0.532	402.24	14.80	12.62	3.18	2.95
BP4	0.652	446.80	63.99	45.54	5.72	3.76
BP5	0.380	258.55	34.40	28.07	3.99	3.08

- For each BPs, signal (s) $=$ Signal-I $+$ Signal-II .

Statistical Significance ($\mathcal{S}$)

- We have used following formula in determining $\mathcal{S}$,

$$\mathcal{S} = \sqrt{2 \times \left[(s+b)\ln\left(1+\frac{s}{b}\right) - s\right]}$$

- $\mathcal{S}$ **for different BPs** :

Signal at 13 TeV		Statitical Significance ($\mathcal{S}$)	Required Luminosity $\mathcal{L}$ (fb^{-1})
BP	DM mass [GeV]	$\mathcal{L} = 100$ fb^{-1}	$\mathcal{S} = 3\sigma$
BP1	87.6	3.5	74.4
BP2	132.0	2.0	223.0
BP3	171.1	1.3	545.3
BP4	86.7	1.8	282.3
BP5	119.0	1.4	473.9

Conclusion - First Part

☺ By introducing singlet fermion, we have overcome the drawbacks of pure triplet fermions.

Conclusion - First Part

- ☺ By introducing singlet fermion, we have overcome the drawbacks of pure triplet fermions.
- ☺ The lightest among the two neutral fermions becomes a viable DM candidate.

Conclusion - First Part

- ☺ By introducing singlet fermion, we have overcome the drawbacks of pure triplet fermions.
- ☺ The lightest among the two neutral fermions becomes a viable DM candidate.
- ☺ DM can be tested in different on going DD experiments like Xenon-1T, LUX.

Conclusion - First Part

- ☺ By introducing singlet fermion, we have overcome the drawbacks of pure triplet fermions.
- ☺ The lightest among the two neutral fermions becomes a viable DM candidate.
- ☺ DM can be tested in different on going DD experiments like Xenon-1T, LUX.
- ☺ Fermi-LAT and HESE can detect the DM indirectly by detecting gamma-rays signal in future.

Conclusion - First Part

- ☺ By introducing singlet fermion, we have overcome the drawbacks of pure triplet fermions.
- ☺ The lightest among the two neutral fermions becomes a viable DM candidate.
- ☺ DM can be tested in different on going DD experiments like Xenon-1T, LUX.
- ☺ Fermi-LAT and HESE can detect the DM indirectly by detecting gamma-rays signal in future.
- ☺ This model can also be tested at collider by searching multi-jet $+ \not{E}_T$ signal.

Non-thermal Dark Matter

- "Explaining the 3.5 keV X-ray Line in a $L_\mu - L_\tau$ Extension of the Inert Doublet Model", A. Biswas, S. Choubey, L. Covi and **S.K.**, JCAP **1802**, no. 02, 002 (2018) [arXiv:1711.00553 [hep-ph]].

Direct Detection Cross section

DM mass vs SI DD cross section

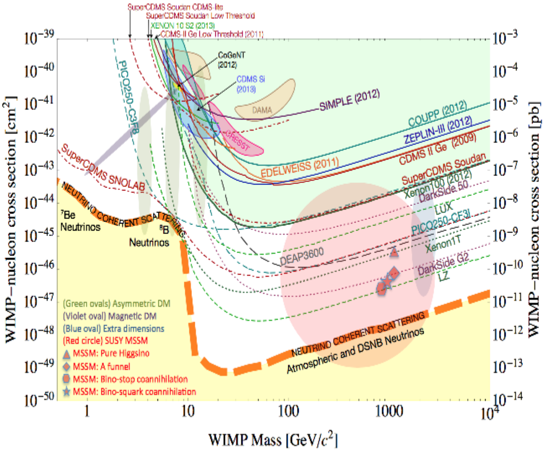

Few words on DD

- So far no DD signal has been observed.

Few words on DD

- So far no DD signal has been observed.
- In near future, SIDD cross section is going to touch neutrino floor.

Few words on DD

- So far no DD signal has been observed.
- In near future, SIDD cross section is going to touch neutrino floor.
- We need to develop our detector to distinguish the DM and neutrino signal.

Few words on DD

- So far no DD signal has been observed.
- In near future, SIDD cross section is going to touch neutrino floor.
- We need to develop our detector to distinguish the DM and neutrino signal.
- To tackle this, we can think of DM production mechanism where SIDD cross section is suppressed by model construction.

Few words on DD

- So far no DD signal has been observed.
- In near future, SIDD cross section is going to touch neutrino floor.
- We need to develop our detector to distinguish the DM and neutrino signal.
- To tackle this, we can think of DM production mechanism where SIDD cross section is suppressed by model construction.
- DM production via Freeze-in mechanism falls in this category. This type of DM never achieve thermal equilibrium hence non-thermal DM.

Freeze-in mechanism [Hall et. al, 09]

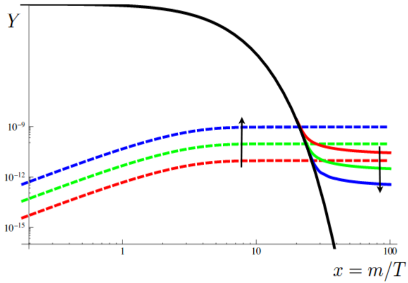

Figure: DM production via freeze-in mechanism.

- DM initial abundance is zero.

Freeze-in mechanism [Hall et. al, 09]

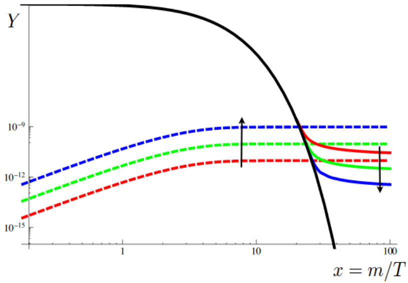

Figure: DM production via freeze-in mechanism.

- DM initial abundance is zero.
- DM relic density is proportional to the coupling strength.

Freeze-in coupling strength [Hall et. al, 09]

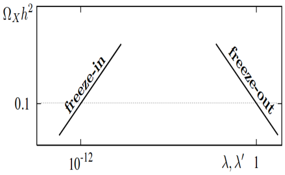

Figure: Freeze-in coupling strength.

- Coupling strength is very feeble, hence feebly interacting massive particle (FIMP).

Freeze-in coupling strength [Hall et. al, 09]

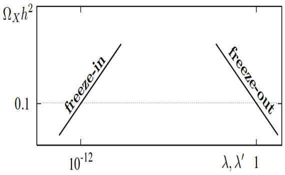

Figure: Freeze-in coupling strength.

- Coupling strength is very feeble, hence feebly interacting massive particle (FIMP).
- Due to such low coupling DM never achieve thermal equilibrium ($\frac{\langle\Gamma\rangle}{H} < 1$), hence it is also called non-thermal DM.

Freeze-in coupling strength [Hall et. al, 09]

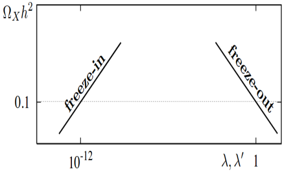

Figure: Freeze-in coupling strength.

- Coupling strength is very feeble, hence feebly interacting massive particle (FIMP).
- Due to such low coupling DM never achieve thermal equilibrium ($\frac{\langle \Gamma \rangle}{H} < 1$), hence it is also called non-thermal DM.
- Also for such low coupling, FIMP DM is safe from all the existing bounds.

Strategy in Non-thermal DM study

Briefly, we obey the following steps:

- Produce the extra gauge boson from the decay of the BSM Higgs.

Strategy in Non-thermal DM study

Briefly, we obey the following steps:

- Produce the extra gauge boson from the decay of the BSM Higgs.
- Produce DM from the decay of extra gauge boson.

Strategy in Non-thermal DM study

Briefly, we obey the following steps:

- Produce the extra gauge boson from the decay of the BSM Higgs.
- Produce DM from the decay of extra gauge boson.
- DM decay which gives 3.55 keV line.

Strategy in Non-thermal DM study

Briefly, we obey the following steps:

- Produce the extra gauge boson from the decay of the BSM Higgs.
- Produce DM from the decay of extra gauge boson.
- DM decay which gives 3.55 keV line.
- In discussing above things, we assume $U(1)_{L_\mu - L_\tau}$ extension with additional particles.

Particle Spectrum

Particles and their charges under SM and $\mathbb{Z}_2$ gauge groups :

Gauge Group	Baryon Fields			Lepton Fields			Scalar Fields		
	$Q_L^i = (u_L^i, d_L^i)^T$	u_R^i	d_R^i	$L_L^i = (\nu_L^i, e_L^i)^T$	e_R^i	N_R^i	ϕ_h	ϕ_H	η
$\mathrm{SU(2)_L}$	2	1	1	2	1	1	2	1	2
$\mathrm{U(1)_Y}$	1/6	2/3	−1/3	−1/2	−1	0	1/2	0	1/2
$\mathbb{Z}_2$	+	+	+	+	+	−	+	+	−

Particles and their charges under $\mathrm{U(1)_{L_\mu - L_\tau}}$ gauge group :

Gauge Group	Baryonic Fields	Lepton Fields			Scalar Fields		
	(Q_L^i, u_R^i, d_R^i)	(L_L^e, e_R, N_R^e)	$(L_L^\mu, \mu_R, N_R^\mu)$	$(L_L^\tau, \tau_R, N_R^\tau)$	ϕ_h	ϕ_H	η
$\mathrm{U(1)}_{L_\mu - L_\tau}$	0	0	1	−1	0	1	0

Lagrangian

- Complete Lagrangian:

$$\mathcal{L} = \mathcal{L}_{SM} + \mathcal{L}_N + (D_\mu \phi_H)^\dagger (D^\mu \phi_H) + (D_\mu \eta)^\dagger (D^\mu \eta) + \sum_{j=\mu,\,\tau} Q^j\, \bar{L}_j \gamma_\rho L_j Z^\rho_{\mu\tau}$$
$$-\frac{1}{4} F_{\mu\tau\,\rho\sigma} F_{\mu\tau}{}^{\rho\sigma} - V(\phi_h, \phi_H, \eta)\,,$$

- Lagrangian for RH neutrinos:

$$\mathcal{L}_N = \sum_{i=e,\,\mu,\,\tau} \frac{i}{2} \bar{N}_i \gamma^\mu D_\mu N_i - \frac{1}{2} M_{ee}\, \bar{N}_e^c N_e - \frac{1}{2} M_{\mu\tau}\, (\bar{N}_\mu^c N_\tau + \bar{N}_\tau^c N_\mu)$$
$$-\frac{1}{2} h_{e\mu} (\bar{N}_e^c N_\mu + \bar{N}_\mu^c N_e) \phi_H^\dagger - \frac{1}{2} h_{e\tau} (\bar{N}_e^c N_\tau + \bar{N}_\tau^c N_e) \phi_H$$
$$- \sum_{\alpha=e,\,\mu,\,\tau} h_\alpha \bar{L}_\alpha \tilde{\eta} N_\alpha + h.c.\,,$$

- Complete potential:

$$V(\phi_h, \phi_H, \eta) = -\mu_H^2 \phi_H^\dagger \phi_H - \mu_h^2 \phi_h^\dagger \phi_h + \mu_\eta^2 \eta^\dagger \eta + \lambda_1 (\phi_h^\dagger \phi_h)^2 + \lambda_2 (\eta^\dagger \eta)^2 + \lambda_3 (\phi_H^\dagger \phi_H)^2$$
$$+\lambda_{12} (\phi_h^\dagger \phi_h)(\eta^\dagger \eta) + \lambda_{13} (\phi_h^\dagger \phi_h)(\phi_H^\dagger \phi_H) + \lambda_{23} (\phi_H^\dagger \phi_H)(\eta^\dagger \eta) + \lambda_4 (\phi_h^\dagger \eta)(\eta^\dagger \phi$$
$$+\frac{1}{2} \lambda_5 \left((\phi_h^\dagger \eta)^2 + h.c. \right)\,.$$

Symmetry break and mass

- Scalars take the following from

$$\phi_h = \begin{pmatrix} 0 \\ \dfrac{v + H}{\sqrt{2}} \end{pmatrix}, \quad \phi_H = \left(\frac{v_{\mu\tau} + H_{\mu\tau}}{\sqrt{2}}\right), \quad \eta = \begin{pmatrix} \eta^+ \\ \dfrac{\eta_R^0 + i\,\eta_I^0}{\sqrt{2}} \end{pmatrix}.$$

- Above vevs, break the symmetry: $\mathrm{SU(2)_L} \times \mathrm{U(1)_Y} \times \mathrm{U(1)_{L_\mu - L_\tau}} \to U(1)_{em}$
- Mass of the Higgses:

$$\begin{aligned}
M^2_{h_1} &= \lambda_1 v^2 + \lambda_3 v^2_{\mu\tau} - \sqrt{(\lambda_3 v^2_{\mu\tau} - \lambda_1 v^2)^2 + (\lambda_{13}\, v\, v_{\mu\tau})^2}\,, \\
M^2_{h_2} &= \lambda_1 v^2 + \lambda_3 v^2_{\mu\tau} + \sqrt{(\lambda_3 v^2_{\mu\tau} - \lambda_1 v^2)^2 + (\lambda_{13}\, v\, v_{\mu\tau})^2}\,, \\
\tan 2\alpha &= \frac{\lambda_{13}\, v_{\mu\tau}\, v}{\lambda_3 v^2_{\mu\tau} - \lambda_1 v^2}\,.
\end{aligned}$$

α is the mixing angle between neutral Higgses.

- Quartic Couplings need to follow the following criterion:

$$
\begin{aligned}
&\lambda_1 \geq 0, \lambda_2 \geq 0, \lambda_3 \geq 0,\\
&\lambda_{12} \geq -2\sqrt{\lambda_1\,\lambda_2},\\
&\lambda_{13} \geq -2\sqrt{\lambda_1\,\lambda_3},\\
&\lambda_{23} \geq -2\sqrt{\lambda_2\,\lambda_3},\\
&\lambda_{12} + \lambda_4 - |\lambda_5| \geq -2\sqrt{\lambda_1\,\lambda_2},\\
&\sqrt{\lambda_{13} + 2\sqrt{\lambda_1\,\lambda_3}}\sqrt{\lambda_{23} + 2\sqrt{\lambda_2\,\lambda_3}}\sqrt{\lambda_{12} + \lambda_4 - |\lambda_5| + 2\sqrt{\lambda_1\,\lambda_2}}\\
&+2\sqrt{\lambda_1\lambda_2\lambda_3} + \lambda_{13}\sqrt{\lambda_2} + \lambda_{23}\sqrt{\lambda_1} + (\lambda_{12} + \lambda_4 - |\lambda_5|)\sqrt{\lambda_3} \geq 0 \quad ,\\
&\sqrt{\lambda_{13} + 2\sqrt{\lambda_1\,\lambda_3}}\sqrt{\lambda_{23} + 2\sqrt{\lambda_2\,\lambda_3}}\sqrt{\lambda_{12} + 2\sqrt{\lambda_1\,\lambda_2}}\\
&+2\sqrt{\lambda_1\lambda_2\lambda_3} + \lambda_{13}\sqrt{\lambda_2} + \lambda_{23}\sqrt{\lambda_1} + \lambda_{12}\sqrt{\lambda_3} \geq 0 \quad .
\end{aligned}
$$

Neutrino mass

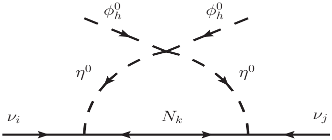

Figure: Neutrino mass generate by the one loop diagram.

- Neutrino mass generated by the one-loop diagram takes the following form,

$$M^{\nu}_{ij} = \sum_k \frac{y_{ik}\, y_{jk}\, M_k}{16\,\pi^2} \left[\frac{M^2_{\eta^0_R}}{M^2_{\eta^0_R} - M^2_k} \ln \frac{M^2_{\eta^0_R}}{M^2_k} - \frac{M^2_{\eta^0_I}}{M^2_{\eta^0_I} - M^2_k} \ln \frac{M^2_{\eta^0_I}}{M^2_k} \right]$$

where $y_{ji} = h_j U_{ji}$ and $N_\alpha = \sum U_{\alpha i} N_i$.

BE for Gauge boson Production

- Boltzmann Equation:

$$\hat{L} f_{Z_{\mu\tau}} = \sum_{i=1,2} \mathcal{C}^{h_i \to Z_{\mu\tau} Z_{\mu\tau}} + \mathcal{C}^{Z_{\mu\tau} \to \, all}$$

BE for Gauge boson Production

- Boltzmann Equation:

$$\hat{L} f_{Z_{\mu\tau}} = \sum_{i=1,2} \mathcal{C}^{h_i \to Z_{\mu\tau} Z_{\mu\tau}} + \mathcal{C}^{Z_{\mu\tau} \to \, all}$$

- For FRW metric, the Lioville's operator takes the following form,

$$\hat{L} = \frac{\partial}{\partial t} - Hp \frac{\partial}{\partial p}$$

BE for Gauge boson Production

- Boltzmann Equation:

$$\hat{L} f_{Z_{\mu\tau}} = \sum_{i=1,2} \mathcal{C}^{h_i \to Z_{\mu\tau} Z_{\mu\tau}} + \mathcal{C}^{Z_{\mu\tau} \to \, all}$$

- For FRW metric, the Lioville's operator takes the following form,

$$\hat{L} = \frac{\partial}{\partial t} - Hp\frac{\partial}{\partial p}$$

- Depends on two variables (T(t),p) and if we define two new variables (ξ_p, r) [J. König et. al., JCAP16], where

$$r = \frac{M_{sc}}{r}, \;\; \xi_p = \mathcal{B}(r)\frac{p}{T}, \;\; \text{and} \;\; \frac{dT}{dt} = -HT\left(1 + \frac{T g_s'(T)}{3 g_s(T)}\right)^{-1}$$

BE for Gauge boson Production

- Boltzmann Equation:

$$\hat{L} f_{Z_{\mu\tau}} = \sum_{i=1,2} \mathcal{C}^{h_i \to Z_{\mu\tau} Z_{\mu\tau}} + \mathcal{C}^{Z_{\mu\tau} \to \, all}$$

- For FRW metric, the Lioville's operator takes the following form,

$$\hat{L} = \frac{\partial}{\partial t} - Hp \frac{\partial}{\partial p}$$

- Depends on two variables (T(t),p) and if we define two new variables (ξ_p, r) [J. König et. al., JCAP16], where

$$r = \frac{M_{sc}}{r}, \ \xi_p = \mathcal{B}(r) \frac{p}{T}, \ \text{and} \ \frac{dT}{dt} = -HT \left(1 + \frac{T g_s'(T)}{3 g_s(T)}\right)^{-1}$$

- Liouville's Operator takes the following form ,

$$\hat{L} = r\, H \left(1 + \frac{T g_s'}{3 g_s}\right)^{-1} \frac{\partial}{\partial\, r} \ \rightarrow \ \text{Dependent on one variable}$$

BE for Non-thermal Dark Matter

- BE for the DM,

$$\frac{dY_{N_j}}{dr} = \frac{V_{ij}\, M_{pl}\, r\, \sqrt{g_\star(r)}}{1.66\, M_{sc}^2\, g_s(r)} \left[\sum_{k=1,2} \sum_{i=1,2,3} \langle \Gamma_{h_k \to N_j\, N_i} \rangle (Y_{h_k} - Y_{N_j} Y_{N_i}) \right] + \frac{V_{ij}\, M_{pl}\, r\, \sqrt{g_\star(r)}}{1.66\, M_{sc}^2\, g_s(r)} \sum_{i=1,2,3} \langle \Gamma_{Z_{\mu\tau} \to N_j N_i} \rangle_{NTH} \left(Y_{Z_{\mu\tau}} - Y_{N_j} Y_{N_i} \right),$$

where $Y_{Z_{\mu\tau}} = \frac{n_{Z_{\mu\tau}}}{s}$ and $s = \frac{2\pi^2}{45} g_s(T)\, T^3$

- BE for the DM,

$$
\begin{aligned}
\frac{dY_{N_j}}{dr} &= \frac{V_{ij}\, M_{pl}\, r\, \sqrt{g_\star(r)}}{1.66\, M_{sc}^2\, g_s(r)} \left[\sum_{k=1,2} \sum_{i=1,2,3} \langle \Gamma_{h_k \to N_j\, N_i} \rangle (Y_{h_k} - Y_{N_j}\, Y_{N_i}) \right] \\
&+ \frac{V_{ij}\, M_{pl}\, r\, \sqrt{g_\star(r)}}{1.66\, M_{sc}^2\, g_s(r)} \sum_{i=1,2,3} \langle \Gamma_{Z_{\mu\tau} \to N_j N_i} \rangle_{NTH} \left(Y_{Z_{\mu\tau}} - Y_{N_j}\, Y_{N_i} \right),
\end{aligned}
$$

where $Y_{Z_{\mu\tau}} = \frac{n_{Z_{\mu\tau}}}{s}$ and $s = \dfrac{2\pi^2}{45}\, g_s(T)\, T^3$

- Number density is given by

$$
n_{Z_{\mu\tau}}(r) = \frac{g\, T^3}{2\pi^2}\, \mathcal{B}(r)^3 \int d\xi_p\, \xi_p^2\, f_{Z_{\mu\tau}}(\xi_p,\, r)\,,
$$

where

$$
\mathcal{B}(r) = \left(\frac{g_s(T_0)}{g_s(T)} \right)^{1/3} = \left(\frac{g_s(M_{sc}/r)}{g_s(M_{sc}/r_0)} \right)^{1/3} .
$$

Contd...

- Thermal average of decay width is defined as,

$$\langle \Gamma_{h_k \to N_j\, N_i} \rangle = \Gamma_{h_k \to N_j\, N_i} \frac{K_1\left(r\,\frac{M_{h_k}}{M_{sc}}\right)}{K_2\left(r\,\frac{M_{h_k}}{M_{sc}}\right)}\,,$$

K_i is the modified Bessel function of i^{th} kind.

Contd...

- Thermal average of decay width is defined as,

$$\langle \Gamma_{h_k \to N_j\, N_i} \rangle = \Gamma_{h_k \to N_j\, N_i} \frac{K_1\left(r\,\frac{M_{h_k}}{M_{sc}}\right)}{K_2\left(r\,\frac{M_{h_k}}{M_{sc}}\right)}\,,$$

  K_i is the modified Bessel function of i^{th} kind.

- Non-thermal average of decay width $Z_{\mu\tau} \to N_j N_i$ is,

$$\langle \Gamma_{Z_{\mu\tau} \to N_j N_i} \rangle_{NTH} = M_{Z_{\mu\tau}} \Gamma_{Z_{\mu\tau} \to N_j N_i} \frac{\int \frac{f_{Z_{\mu\tau}}(p)}{\sqrt{p^2 + M^2_{Z_{\mu\tau}}}} d^3p}{\int f_{Z_{\mu\tau}}(p) d^3p}\,,$$

  $f_{Z_{\mu\tau}}$ is the non-thermal distribution of $Z_{\mu\tau}$.

Gauge boson distribution function

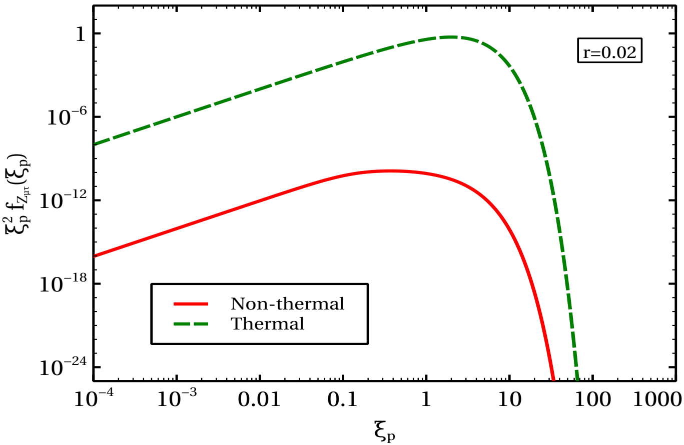

Figure: Thermal and Non-thermal distribution function of $Z_{\mu\tau}$ gauge boson.

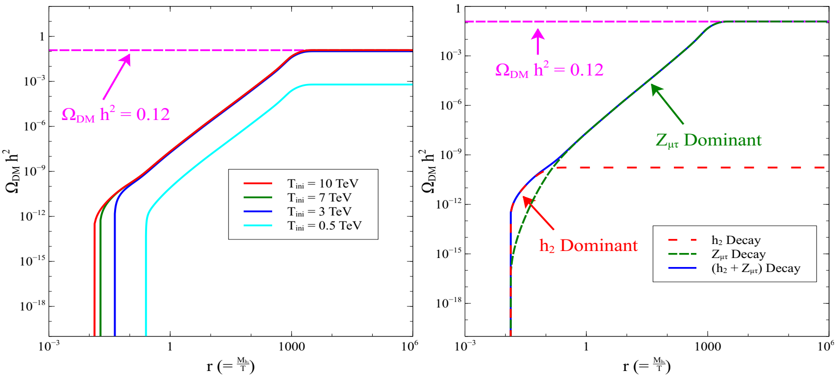

Figure: Variation of relic density with r where other parameters are fixed at $g_{\mu\tau} = 1.01 \times 10^{-11}$, $\alpha = 0.01$, $M_{Z_{\mu\tau}} = 1$ TeV, $M_{DM} = 100$ GeV, $M_{h_2} = 5$ TeV and $M_{N_1} = 150$ GeV and $M_{DM} = M_{N_2} \simeq M_{N_3} = 100$ GeV.

Contd..

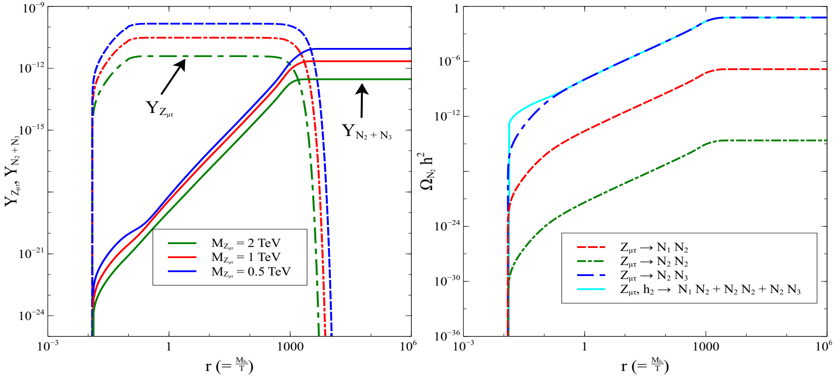

Figure: Variation of relic density with r where other parameters are fixed at $g_{\mu\tau} = 1.01 \times 10^{-11}$, $\alpha = 0.01$, $M_{Z_{\mu\tau}} = 1$ TeV, $M_{DM} = 100$ GeV, $M_{h_2} = 5$ TeV and $M_{N_1} = 150$ GeV and $M_{DM} = M_{N_2} \simeq M_{N_3} = 100$ GeV.

3.55 keV γ-ray line

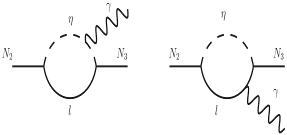

Figure: Diagrams for 3.55 keV γ-ray line.

- Flux expression takes the following form,

$$\Phi = \frac{1}{4\pi M_{N_2} \tau_{N_2}} \int_{l.o.s.} \rho_{N_2}(\vec{r}) d\vec{r}$$

  where τ_{N_2}: DM decay life, ρ_{N_2}: DM halo density.

- Constraint on decay width to explain 3.55 keV line is,

$$\Gamma(N_2 \to N_3\gamma) \quad = \quad (0.2 - 1.9) \times 10^{-44}\,\mathrm{GeV} \left(\frac{M_{N_2}}{100\,\mathrm{GeV}}\right).$$

- If N_2 and N_3 have opposite parity then, $N_2 \to N_3\gamma$ happen by the magnetic moment term generated at the one loop level [Pal et. al, PRD 82].
- Decay rate is:

$$\Gamma(N_2 \to N_3\gamma) = \frac{\mu_{23}^2}{4\pi}\,\delta^3\,\left(1 - P\,\frac{M_{N_3}}{M_{N_2}}\right)^2$$

where

$$\mu_{23} = \sum_i \frac{e}{2}\frac{1}{(4\pi)^2}\frac{M_{N_2}}{M_\eta^2}(y_{i2}y_{i3})\,,\quad \delta = \frac{M_{N_2}}{2}\left(1 - \frac{M_{N_3}^2}{M_{N_2}^2}\right)\,,\quad P = \pm 1$$

- For $M_\eta = 10^6\,\mathrm{GeV}, M_{N_2} = 100\,\mathrm{GeV}, (y_{ij})^2 = 10^{-1}$, we get $\Gamma_{N_2} \sim 10^{-44}$ GeV, which can explain 3.55 keV line.

Conclusion

- Present model generate the neutrino mass via one loop diagram.
- Dark matter can be produced by the freeze-in mechanism in the right ball-park value put by Planck.
- 3.55 keV line can also be explained by the DM decay.


Thank you